The distribution of dust in edge-on galaxies: I. The global structure

Aleksandr V. Mosenkov [1,2]★ Pavel A. Usachev,[2,3,4] Zacory Shakespear,[1] Jacob Guerrette,[1] Maarten Baes [5] Simone Bianchi,[6] Emmanuel M. Xilouris,[7] George A. Gontcharov [2] Vladimir B. Il'in [2,3,8] Alexander A. Marchuk [2,3] Sergey S. Savchenko[2,3,4] and Anton A. Smirnov[2,3]

Speaker： 闫冰

Date： 2024/5/10

CONTENT

Introduction

1. Introduction

infer the overall spatial distribution of dust in galaxies
by fitting optical images of edge-on galaxies with a prominent dust lane using RT simulations.
In RT modelling, it is generally assumed that dust follows an exponential distribution both in the radial and vertical directions.   -----but the pure exponential decline of the radial and vertical dust profile is not entirely correct

Dozens of nearby edge-on galaxies offer the best opportunity for exploring both the radial and vertical distributions of stars, gas, and dust in great detail.
The natural and most common approach for studying the dust distribution in edge-on galaxies is by exploiting and analysing FIR/submm observations of the thermal emission of dust.
There is now ample evidence for the presence of extraplanar clouds and filaments of dust in disc galaxies.

1. Introduction

- the first systematic study for probing the 3D distribution of dust emission and exploring the general scaling relations between the stellar and dust structural parameters.

Bocchio et al. (2016a) has explored the vertical extent of dust emission around NGC 0891 and revealed the presence of a second, thick dust disc component.

- expand their study and demonstrate the existence of extraplanar FIR emission in other nearby, well-resolved edge-on galaxies.
- study the distribution of the FIR/submm emission, which is not the same as the mass-density distribution of dust.

The monochromatic luminosity density distribution can be approximated by a modified blackbody (MBB) model written as

$$I_\nu(\lambda) = \kappa(\lambda_0) \sum_d \left(\frac{\lambda_0}{\lambda}\right)^\beta B_\nu(T_d, \lambda)$$

assume that β and $\kappa(\lambda_0)$ do not vary significantly inside the galaxy
the constructed mass density profiles of cold dust in galaxies generally follow the FIR/submm luminosity density distribution

In this paper by the dust distribution they mean the FIR surface brightness distribution.

The Data and Sample

2. The Data and Sample

exploit the DustPedia imagery (including the error maps) in the five *Herschel* bands.

Waveband	Pixel scale (arcsec)	Point spread function(PSF) FWHM (arcsec)
PACS 100	3	8
PACS 160	4	12
SPIRE 250	6	18
SPIRE 350	8	24
SPIRE 500	12	36

From the whole DustPedia sample, they pre-selected **50 edge-on galaxies** based on the galaxy inclination angle $i \geq 85°$ estimated in Mosenkov et al.(2019, hereafter M19). rejected galaxies
- in which the disc is obviously less inclined so that the spirals are well-seen
- have a deformed, irregular shape
- with a radial extent of less than 2 arcmin in the PACS 100 band
- with a vertical extent of a few pixels only

a final sample of **29 genuine edge-on galaxies** with an inclination angle $i \gtrsim 85°$.
split by hand the final sample into two subsamples: the main sample (D25 $\gtrsim$ 4 arcmin, 16 galaxies) and the additional sample (D25 $\lesssim$ 4 arcmin, 13 galaxies).

2. The Data and Sample

list the general properties of the galaxies under study in Table 1

the galaxies in the sample are nearby, have a large angular extent, and are mostly of type Sb–Sc span fairly wide ranges of stellar masses($9 \lesssim \log M_*/M_\odot \lesssim 11$), dust masses ($6 \lesssim \log M_{dust}/M_\odot \lesssim 8$), and maximum rotation velocities ($70 \ km \ s^{-1} \lesssim v_{rot} \lesssim 300 \ km \ s^{-1}$).

Table 1. The general properties of edge-on galaxies from the main (upper part) and additional (bottom part) samples.

Galaxy	RA (J2000)	Dec. (J2000)	D (Mpc) (1)	D25 (arcmin) (2)	$\log M_*$ ($M_\odot$) (3)	Type (4)	i (deg) (5)	Ref. (6)	v_{rot} (km s^{-1}) (7)	$\log M_{dust}$ ($M_\odot$) (8)
ESO 209-009	07:58:15	−49:51:15	12.59	6.49	10.12	SBc	87.1 ± 1.5	this study*	141.4 ± 3.6	7.21 ± 0.05
ESO 373-008	09:33:22	−33:02:01	9.68	3.7	9.56	Sc	89.5 ± 1.5	this study*	93.7 ± 2.8	6.7 ± 0.06
IC 2531	09:59:56	−29:37:01	36.65	6.53	10.83	Sc	89.5 ± 0.2	1,2,3	228.3 ± 3.2	7.75 ± 0.06
NGC 0891	02:22:33	+ 42:20:57	9.86	13.03	10.82	Sb	89.7 ± 0.3	1,4,5	212.1 ± 5.0	7.7 ± 0.05
NGC 3628	11:20:17	+ 13:35:23	10.81	11.04	10.82	SBb	88.4 ± 1.5	5	212.1 ± 3.4	7.61 ± 0.05

2. The Data and Sample

To trace the old stellar population in the galaxies (which makes up the bulk of the stellar mass), they use the 3.4 μm (W1) imaging available thanks to the WISE space observatory. The pixel size is 1.375 arcsec and FWHM = 6.1 arcsec.

The reason why they use *WISE* data
- all galaxies in our sample are imaged by *WISE*
- the poor *WISE* resolution is more compatible with the *Herschel* resolution as fine structural details in the large nearby galaxies are smeared out and their global stellar structure (decomposed into a single disc and a bulge) can be easily compared to the dust structure traced by *Herschel* .

Data Preparation

PART.03

3. Data Preparation

- for each galaxy image, examine the background emission to remove extrinsic sources.
  > To mask out all objects, including the target galaxy, they employed `SExtractor` (Bertin & Arnouts 1996) with the parameters `DETECT THRESH = 2.0` and `DETECT MINAREA = 3`.
  > The size of the created mask was enlarged by a factor of 1.5, as determined empirically, to totally cover all scattered light.
- all the *Herschel* galaxy images were rebinned to the PACS 100 image.
- all galaxy images were rotated by an average angle estimated by M19.
- in our final images the galactic discs are aligned with the horizontal direction.
- cropped the images for each galaxy, so that the final frames in all five bands would have the same size.
- The rebinning, rotation, and cropping procedures were also applied to the error maps which contain information about the weight for each pixel as a measure of the photometric quality.

Finally, for each galaxy they created a unified mask image consisting of a sum of the individual masks in each band which they initially created for the background subtraction.

The Fitting Method

PART.04

4. The Fitting Method

Using a single Sersic model, M19 performed 2D fitting of cold dust emission profiles for 320 DustPedia galaxies, including all objects from this sample.
modify the modelling approach which was applied in M19 in several aspects.

- in contrast to M19 , who used automatic image preparation for galaxy fitting, the background subtraction and masking in this study were revised to accurately account for all possible sources that could potentially contaminate the galaxy emission.
- for galaxies with bright FIR emission clumps or other unresolved components located in the plane of the galaxy, these features are fitted using a Gaussian or Sersic function. This is done to minimize the influence of such compact sources on the overall galaxy profile instead of masking them out.
- use two alternative models in this study: a simple Sersic model and a 3D broken exponential disc(introduce them in Sections 4.1 and 4,2)
- employ the IMFIT code (Erwin 2015) instead of GALFIT (Peng et al. 2002 , 2010) and GALFITM (Bamford et al. 2011 ; Ha¨ußler et al. 2013), which were used in M19 . This is done because the latter two codes do not include 3D fitting models.

4. The Fitting Method

4.1. Sersic model

The Sersic function is characterized by the following major-axis intensity profile:

$$I(r) = I_e \exp\left\{-b_n\left[\left(\frac{r}{r_e}\right)^{\frac{1}{n}} - 1\right]\right\}$$

where r is the radius, I_e is the surface brightness at the effective (half-light) radius r_e , and the Sersic index n controls the shape of the intensity profile. The function b_n is calculated via the polynomial approximation found by Ciotti & Bertin (1999) (when $n > 0.36$) and MacArthur, Courteau & Holtzman (2003) (when $n \leq 0.36$).

- For **galaxies from the main sample**

start fitting with a 250 μm galaxy image.   ---- it has an average resolution among the five *Herschel* bands considered and negligible contamination of the warm dust emission as compared to the PACS bands with higher resolution.

the derived n parameter is then kept fixed during the fitting of the galaxy images in the remaining bands.   ------- according to M19, the Sersic index of the dust emission in the 100–500 μm wavebands varies within 10–15 percent of the average value without any systematics with wavelength, and, thus, can be taken independent of wavelength.

- For **galaxies from the additional sample**

the fitting is done in only one PACS 100 waveband.   ---- these galaxies have a lower spatial resolution

4. The Fitting Method

4.2 3D disc model

3D luminosity density model for an axisymmetric disc, the vertical Z-axis of which is inclined by the angle i to the line of sight.
The radial profile in this model is a broken exponential function (Freeman 1970) and the vertical profile has a simple exponential decline.
The 3D luminosity density model $j(R, z)$ *at radius R from the central axis and at height z from the galaxy mid-plane is given by* $j(\mathbf{R}, \mathbf{z}) = j_{rad}(\mathbf{R})e^{-|z|/h_z}$*, where* h_z *is the vertical scale height of the disc.*
The radial distribution in the disc plane is described by

$$j_{rad}(R) = S\, j_0\, e^{-R/h_{in}}[1 + e^{\alpha(R-R_b)}]^{\frac{1}{\alpha}(\frac{1}{h_{in}} - \frac{1}{h_{out}})}, \text{ where } j_0 \text{ is the central luminosity density,}$$

h_{in} *is the exponential scale length of the inner disc region before the break at the radius* R_b, *and* h_{out} *is the exponential scale length of the outer disc region beyond the break radius. The parameter* α *controls the abruptness of the transition between the inner and outer regions of the disc.*
If the 3D luminosity density distribution has no break along the radial profile, then it can be given by

$$j(\mathbf{R}, \mathbf{z}) = J_0 e^{-R/h_R - |z|/h_z}$$

The fitting process is the same as the Sersic model.

Results

5. Results

5.1 Notes on the fit results

For the whole sample , find a reduced $\chi^2 = 1.04 \pm 0.45$ for the 3D disc models and 0.97 ± 0.44 for the Sersic models in all *Herschel* bands under study. These similar values of the reduced χ^2 suggest that both models are almost equally good in describing the 2D galaxy profiles.

According to the results of the modelling of the *Herschel* images, not all galaxies in main and additional samples have reliable values of the apparent flattening and, consequently, the disc scale height in the wavebands.

For some galaxies, the FWHM of the vertical cumulative profile is closely or almost completely aligned with the PSF profile so that the shape of the inner part of the vertical galaxy profile is virtually described by the PSF shape.

not consider such galaxies in statistics and scaling relations in Section 6.

5. Results

5.2 Validity of the results

In Fig. 2 , compare the results of Sersic fitting in this work with those presented in M19 for the same edge-on galaxies.

- The fluxes are in almost perfect agreement (the Pearson correlation coefficient $\varrho = 0.99$)
- For the effective radius, the agreement is excellent ($\varrho = 0.97$).
- The Sersic index is the most sensitive parameter in our fitting, but even for it, a strong correlation ($\varrho = 0.89$) with a few outliers is seen.
- As to the apparent flattening, most galaxies have consistent values in both sets of Sersic models
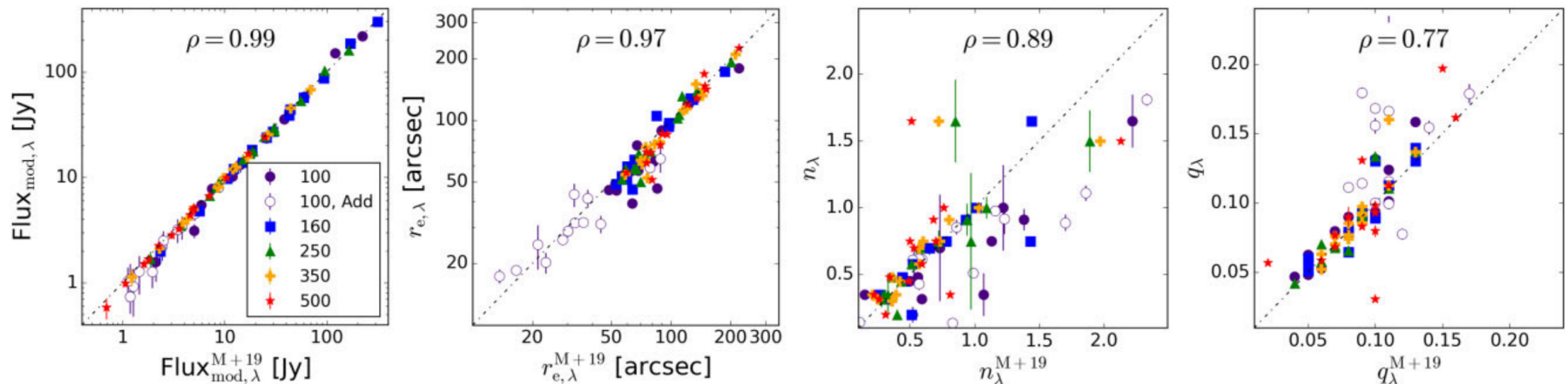
Figure 2. Comparison of the best-fitting parameters for the models obtained in M19 (X-axis) and those obtained in this work (Y-axis) for the Sérsic model. The results for the different bands are depicted by different symbols and colours. The dot-dashed lines show one-to-one relations.

5. Results

5.2 Validity of the results

In Fig. 3 , validate fitting results for the 3D disc models as compared to the Sersic models. both models agree fairly well with few exceptions.
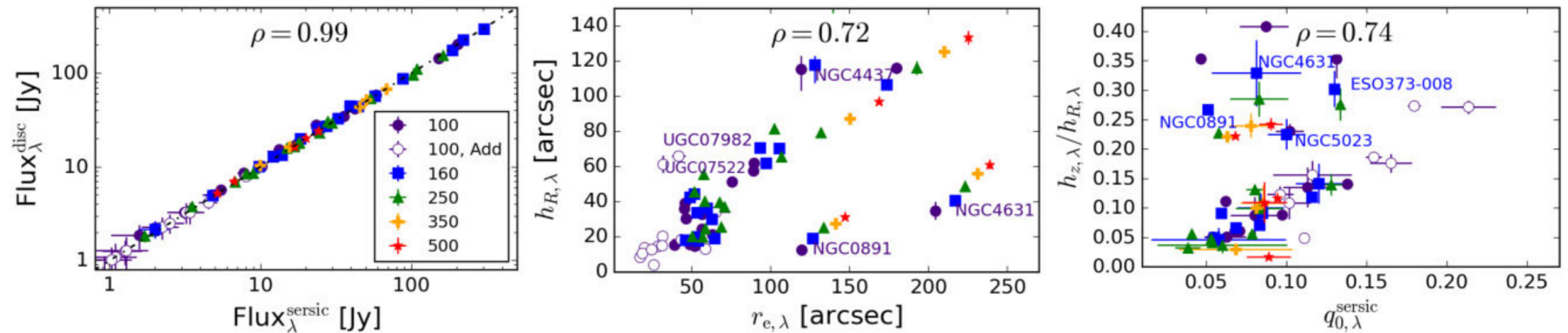

Figure 3. Left-hand panel: Comparison of the 3D disc and Sérsic model fluxes within apertures with the semimajor and semiminor axes from Clark et al. (2018). Middle: Comparison of the 3D disc scale length and the effective radius of the Sérsic model. Right-hand panel: Comparison of the disc scale length-to-scale height ratio versus the intrinsic flattening for the Sérsic model. The dot-dashed line shows a one-to-one relation.

5. Results

5.2 Validity of the results

Fig. 4 presents the comparison of 3D disc models in this work with Sersic models from M19 for the *WISE* 3.4 µm data. As can be seen, the fluxes and geometrical parameters of the models are in good agreement, except for several outliers.

Both NGC 3454 and NGC 4330 have puffed-up stellar discs with boxy isophotes which may explain why these galaxies do not follow the general trend between the intrinsic disc and Sersic flattenings.
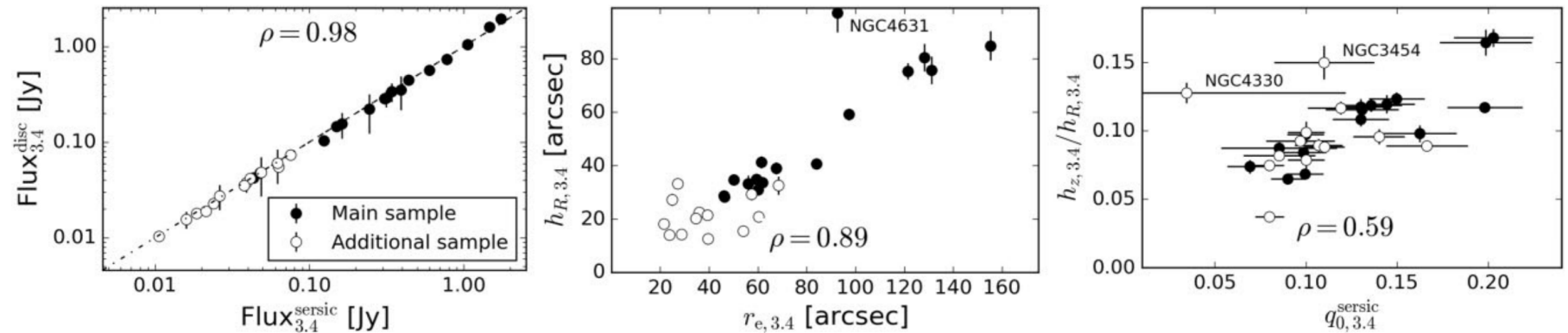

Figure 4. Comparison of the 3D disc model obtained in this study with the Sérsic model from M19 for 3.4 µm data: the model fluxes (left-hand panel), the disc scale length versus the Sérsic effective radius (middle), and the disc relative thickness versus the intrinsic flattening for the Sérsic model (right-hand panel). The dot-dashed line shows a one-to-one relation.

5. Results

5.3 Cumulative intensity profiles

17 galaxies out of 29 demonstrate a noticeable break in their radial profiles
M19 studied the distribution of such characteristic (break) radii for a large sample of
DustPedia galaxies and found a bimodal distribution with one peak centred at $\sim(0.3-0.4)$
$R25$ and another at $\sim 0.6\ R25$, where R25 is half of the optical diameter D25.

- the shorter break radii denote the region where the dust emission deficit should be observed. FIR surface brightness profiles without a depression in the centre are mostly found in galaxies with enhanced star formation in the central region which can be related to **bar instability, formation of a pseudobulge, or AGN activity.**

- the longer break radii beyond $\sim 0.5\ R25$ characterize a smooth transition between the inner profile with a larger scale length and the outer region with a smaller scale length.
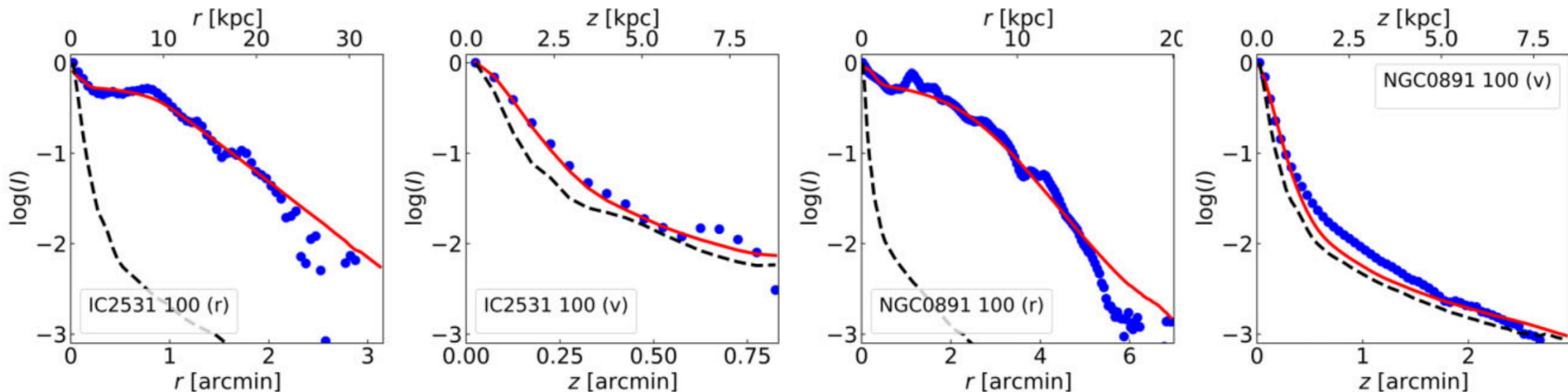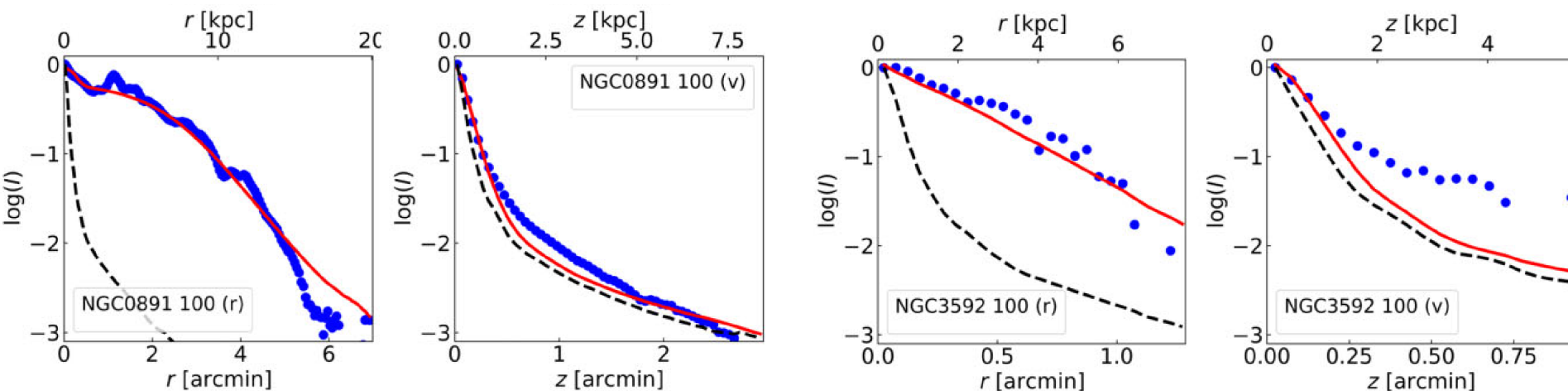
5. Results

5.3 Cumulative intensity profiles

Among 16 galaxies in the main sample, 10 galaxies have additional components apart from the dust disc
(bright clumps, bright central point sources, bulges, and bars)
For example, NGC 0891 has a bright Gaussian source at the centre that is probably related to the bulge or a bar.
Galaxies in the additional sample exhibit smoother profiles due to the worse spatial resolution and thus are only fitted with a single disc component.
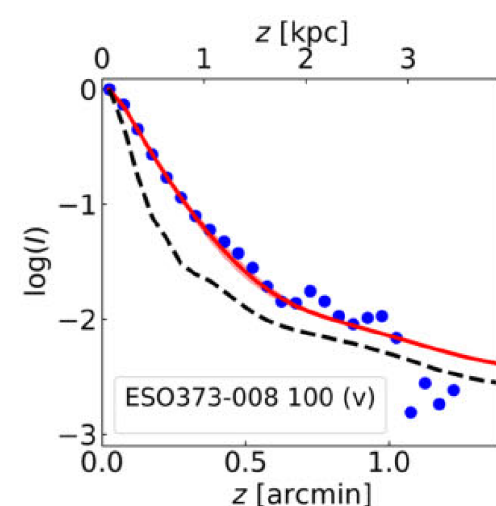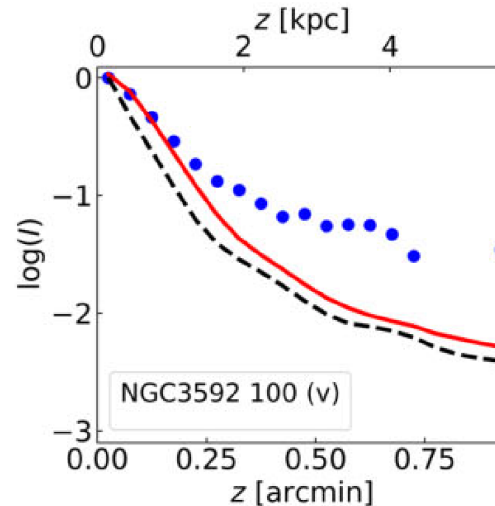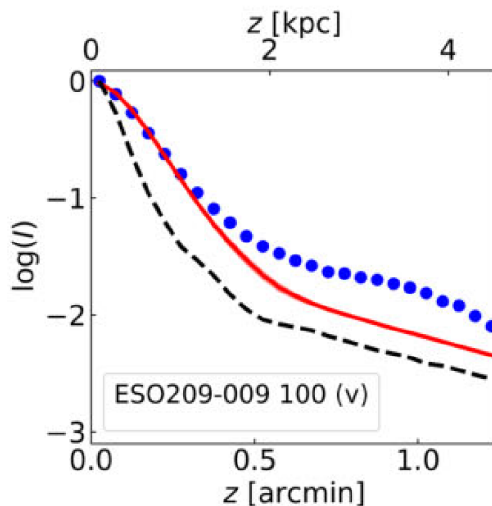
5. Results

5.3 Cumulative intensity profiles

- The vertical profiles for 6 galaxies in main sample show the presence of another (thicker) dust emission component in all or almost all wavebands.
- Six galaxies from the additional sample also show an excess of FIR emission compared to our models at large vertical distances.

They note that this extraplanar FIR emission, which typically starts to dominate at heights 1–2 kpc above the mid-plane, cannot be explained by the scattered light of the PSF.

This indicates that the observed extraplanar emission is produced by the dust at high distances above the mid-plane.

4 galaxies from the main sample show bumps in their cumulative vertical profiles above the model profile which can point to the existence of another vertically extended component.
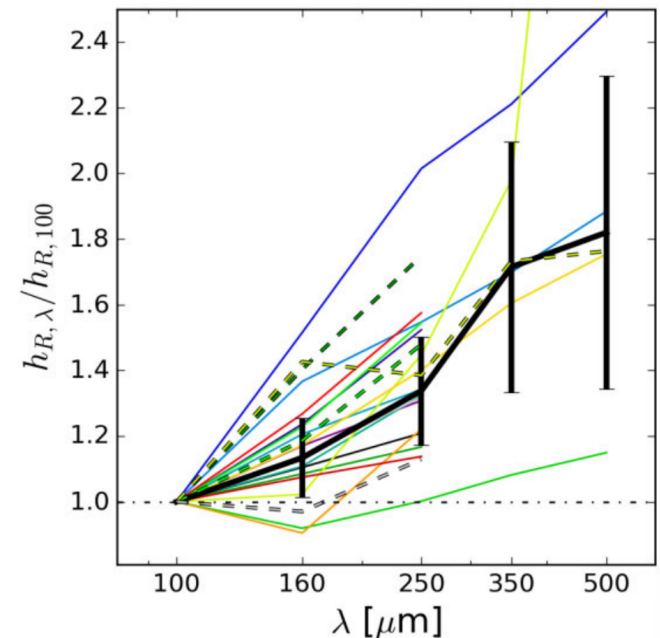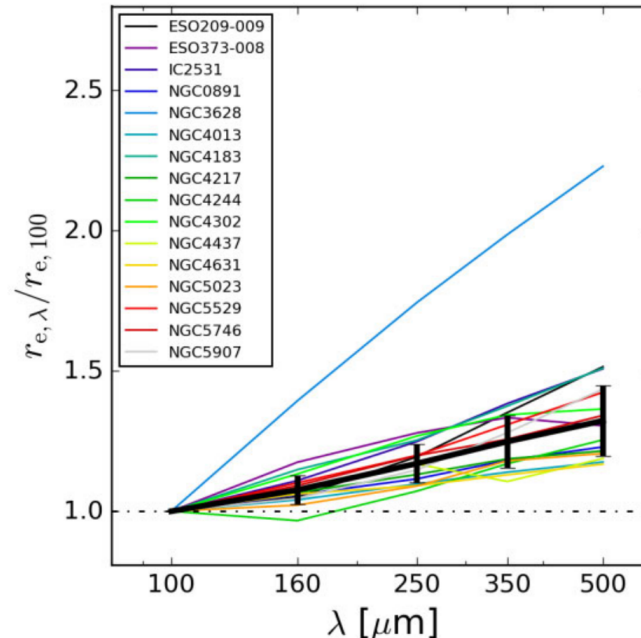
5. Results

5.4 Dependence of the structural parameters on wavelength

In Fig. 6 , they showcase how the structural parameters change with wavelength for both the Sersic and 3D disc models.

- The effective radius, on average, increases up to 30 percent from PACS 100 to SPIRE 500
- A similar positive gradient is found for the disc scale length. The dashed lines depict the change of the scale length for the outer part of the disc (h_{out}) after the break. The outer disc scale length also increases in the same way as the inner scale length.

the observed steady increase of the effective radius and the scale length with wavelength in the FIR domain is related to the dust heating by the diffuse ISRF which is gradually decreasing with radius.

5 Results

5.4 Dependence of the structural parameters on wavelength

In Fig. 6 , they showcase how the structural parameters change with wavelength for both the Sersic and 3D disc models.

- the apparent flattening of the emission profiles does not change significantly with wavelength (within 10 percent, within the uncertainty of this parameter). This suggests that the scale height of the dust emission profile should increase with wavelength.

- the dependence of the disc scale height on wavelength from our 3D disc modelling also confirms this view. Most galaxies demonstrate a gradual increase of the dust disc thickness with wavelength.
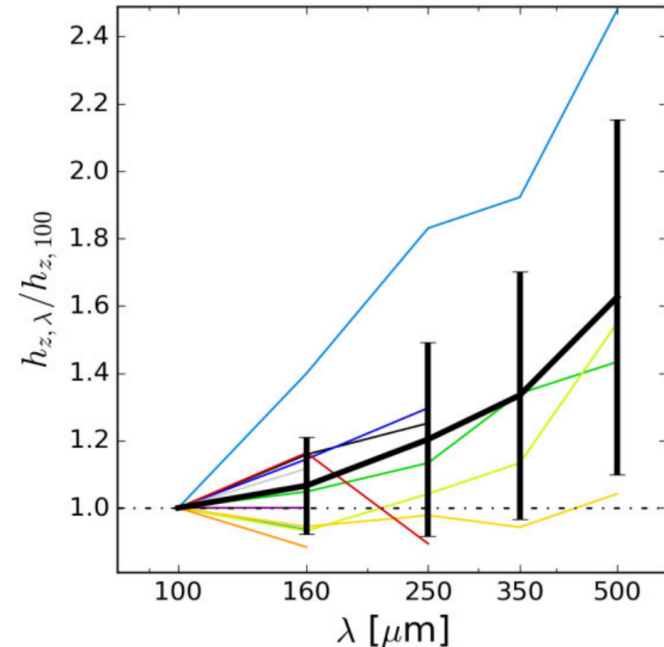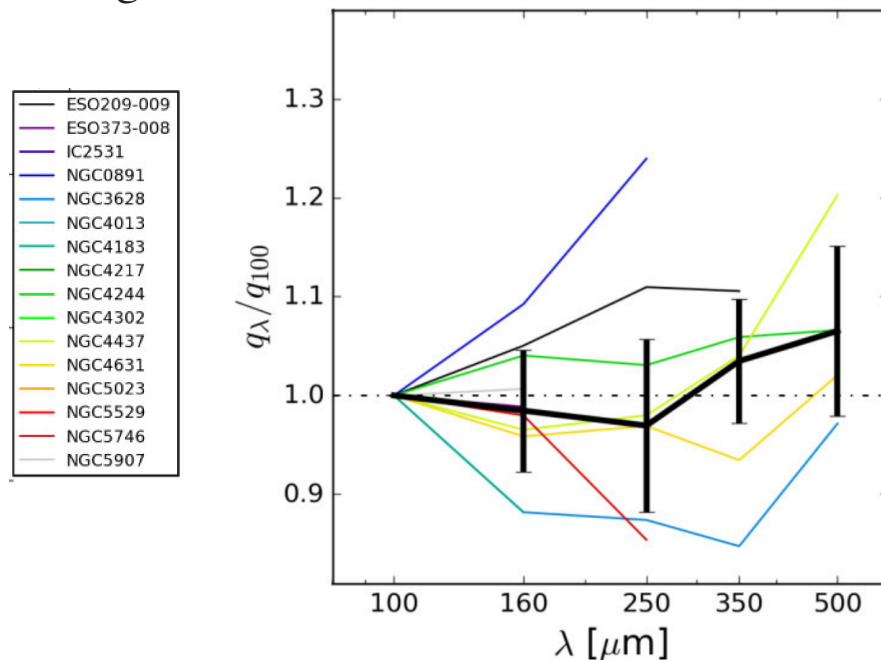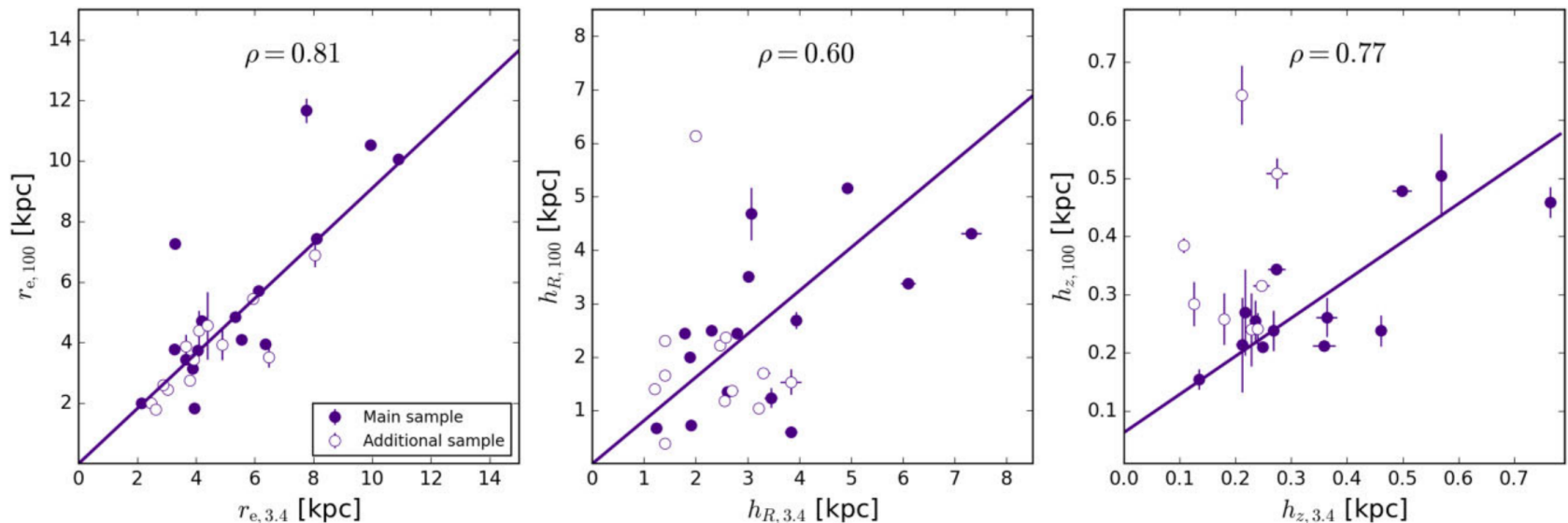
Scaling Relations

6. Scaling Relations

6.1 Dust versus stellar structural parameters

Fig. 7 shows how the dust and stellar radial and vertical scales correlate with each other. the effective radii, the radial scale length and disc scale heights at 100 and 3.4 μm agree very well ($\rho = 0.81, 0.60, 0.77$).

- more extended stellar discs host more extended dust discs.
- the thicker the stellar disc, the thicker the dust disc, on average.

However, there are some obvious outliers, mostly low-mass galaxies from the additional sample, which do not follow this relation.
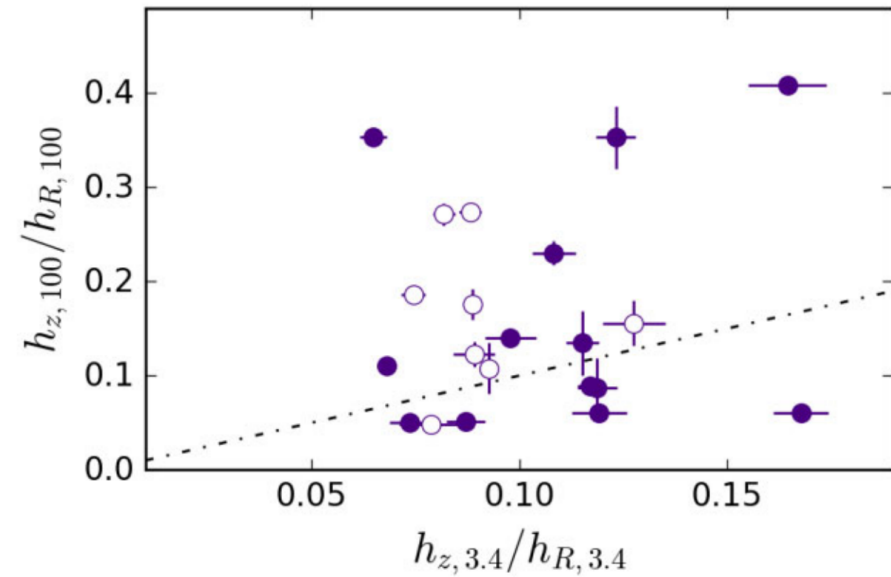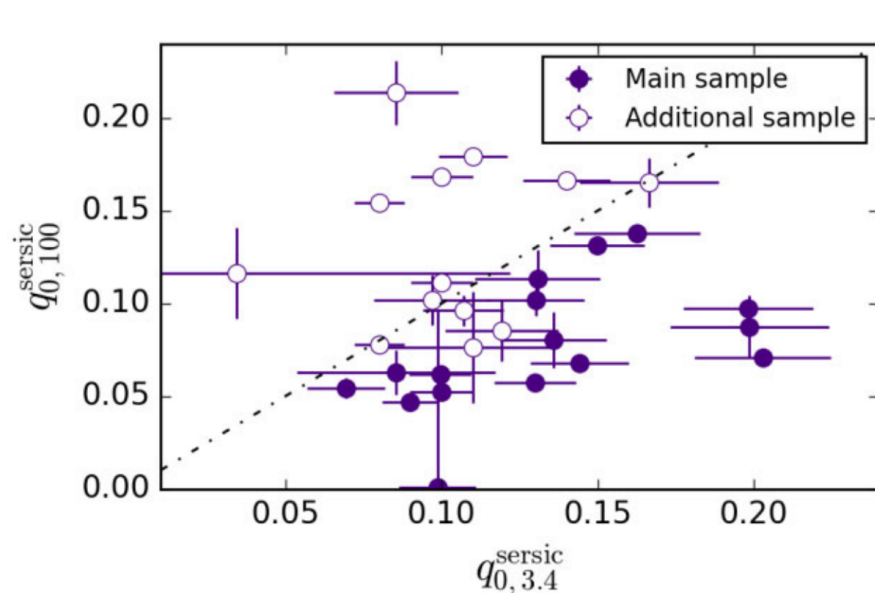
6. Scaling Relations

6.1 Dust versus stellar structural parameters

The intrinsic flattening of the dust disc does not correlate with the intrinsic flattening of the stellar disc, based on both the Sersic and 3D disc models (see Fig. 8).
This indicates that the relative thickness of the dust disc can be rather different from the relative thickness of the stellar disc.
For some dust discs, the relative thickness $h_{z,100}/h_{R,100}$ is exceptionally large and reaches 0.3–0.4 versus $h_{z,3.4}/h_{R,3.4} = 0.1 - 0.15$ for the stellar disc.

6. Scaling Relations

6.1 Dust versus stellar structural parameters

In Fig. 9 we can see the dependence of the disc scale height on the radial scale length for both the 3.4 and 100 μm models. This is a typical scaling relation between the geometrical scales of spiral galaxies: the larger the galaxy in the radial direction, the thicker, on average, it should be.

Both the dust and stellar discs from our sample follow similar relations linking the scale length and scale height ($\rho = 0.51$, with slope $k = 0.098$ and $\rho = 0.85$, with slope $k = 0.103$, respectively).
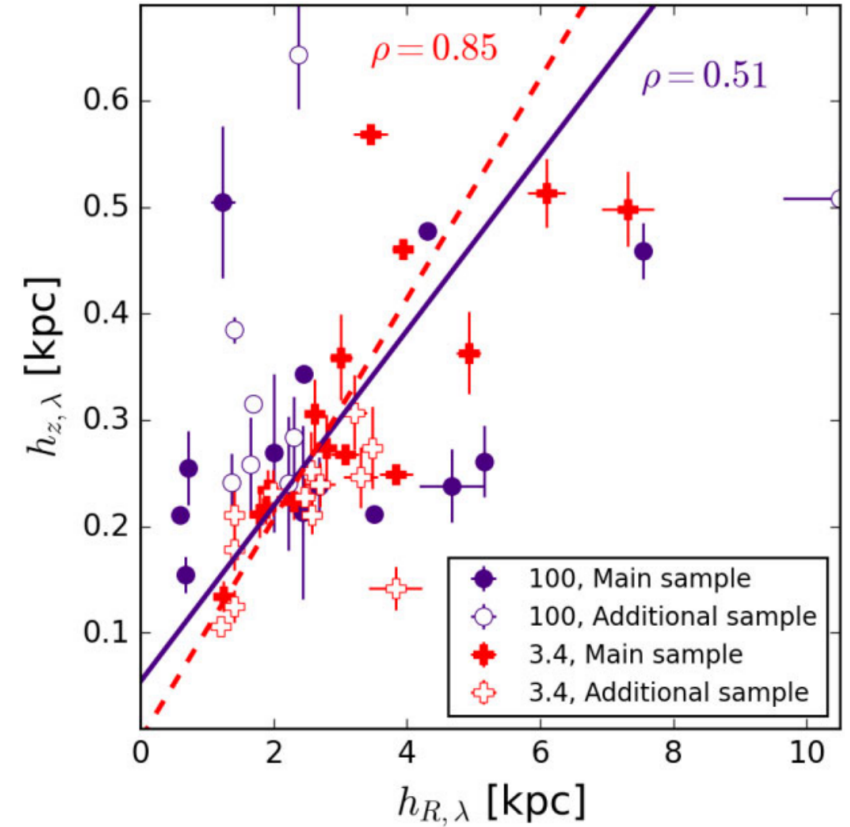

Figure 9. Relation between the disc scale length and scale height at both 3.4 and 100 μm. The thick solid line depicts the linear regression line for the 100 μm data, whereas the red dashed line corresponds to the linear regression fit for 165 edge-on galaxies in the K_s band from Mosenkov et al. (2010).

6. Scaling Relations

6.2 Dust mass–size relation

In Fig. 10 , the dependence of the dust mass on the effective radius for the Sersic model (left-hand panel) and the scale length (middle), and scale height (right-hand panel) for the 3D disc model.
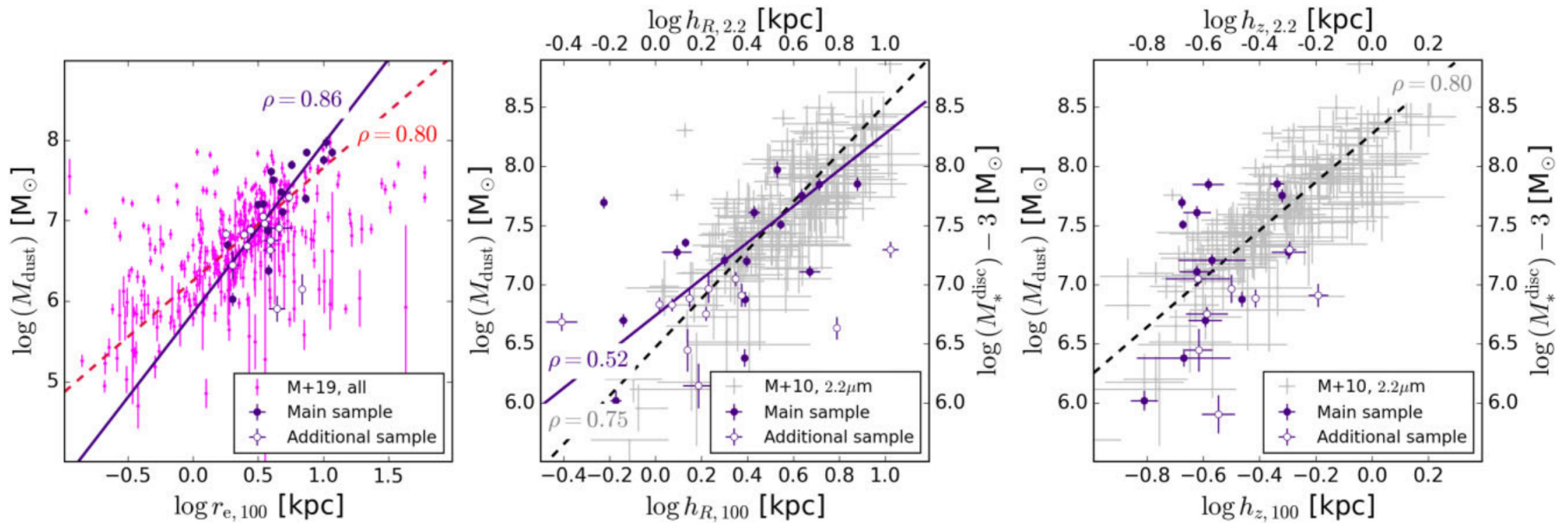

Figure 10. Dependences between the total dust mass from Nersesian et al. (2019) on the Sérsic effective radius (left-hand panel), disc scale length (middle), and disc scale height (right-hand panel) – all for 100 μm. In the left-hand panel we also show galaxies from the whole DustPedia sample in the same PACS 100 waveband. In the middle and right-hand panels, we also display the scaling relations for the stellar discs from Mosenkov et al. (2010) in the 2MASS K_s (2.2 μm) band. The stellar masses are shifted downwards by 3 dex in both plots. The dashed lines are linear regression lines for the large samples of galaxies, whereas the solid lines represent linear regression lines for our samples.

6. Scaling Relations

6.3 Flattening of the dust disc

Fig. 11 shows the intrinsic flattening for the Sersic (left-hand panel) and 3D disc (middle panel) models as well as the ratio of the disc scale height to scale length (right-hand panel).

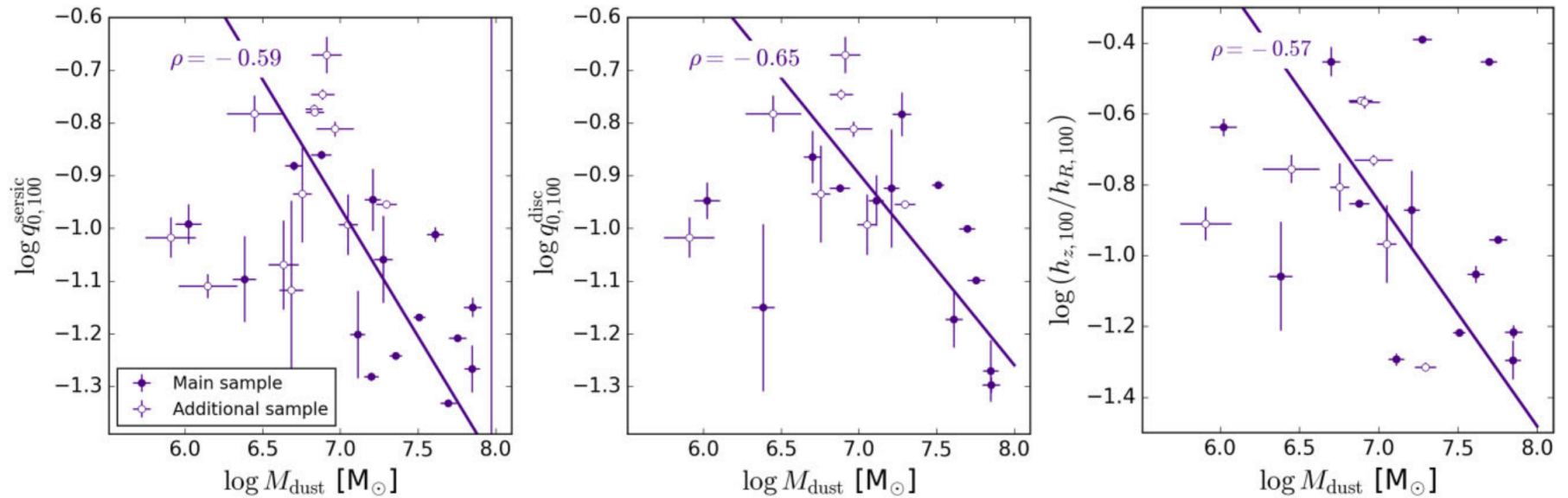**more massive dust discs tend to be flatter**

Figure 11. Dependences between the total dust mass from Nersesian et al. (2019) on the intrinsic flattening for the Sérsic (left-hand panel) and 3D disc (middle) models and the disc scale height-to-length ratio (right-hand panel). The solid lines depict linear regression lines.

6. Scaling Relations

6.3 Flattening of the dust disc

The relative thickness of the disc and the maximum rotation velocity of the galaxy also negatively correlate with each other (see Fig. 12).

flatter dust discs tend to be found in more massive spiral galaxies compared to relatively thick diffuse dust discs in less massive galaxies
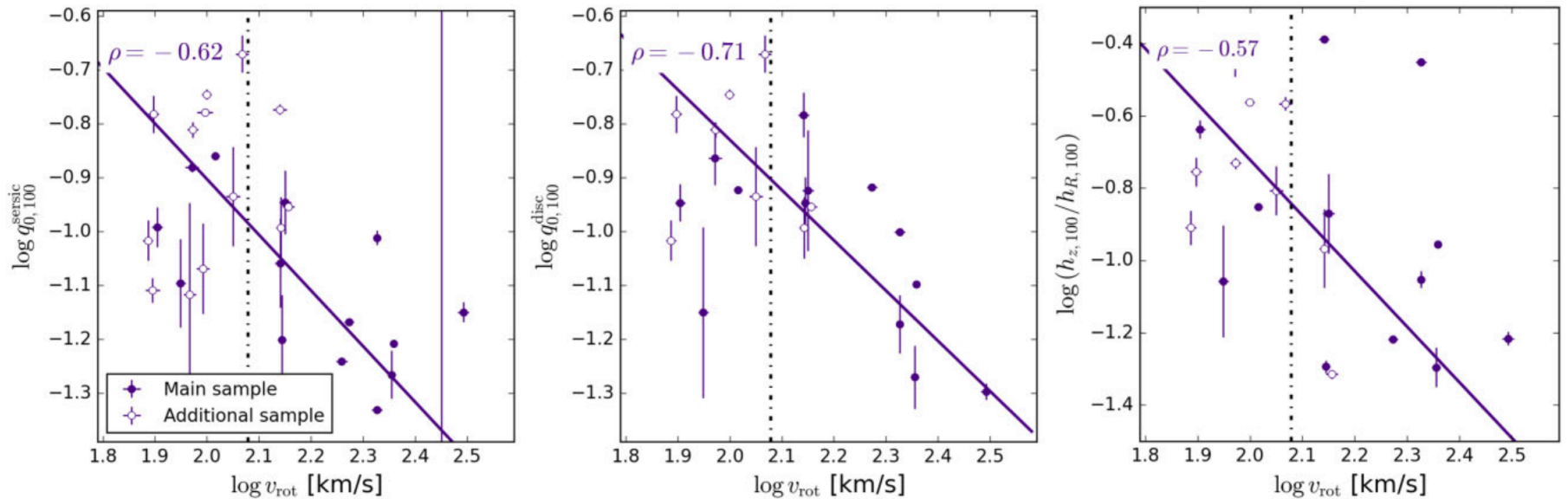

Figure 12. Dependences between the rotation velocity from HyperLeda and the intrinsic flattening for the Sérsic (left-hand panel) and disc (middle) models and the disc scale height-to-length ratio (right-hand panel). The solid lines depict linear regression lines. The dash-dotted lines show $120 \, \mathrm{km\,s^{-1}}$.

6. Scaling Relations

6.3 Flattening of the dust disc

The ratio between the scale height of the dust disc and that of the stellar disc also negatively correlates with the dust mass and maximum rotation velocity (see Fig. 13).
in low-mass galaxies the dust is relatively more distributed throughout the height of the hosting stellar disc
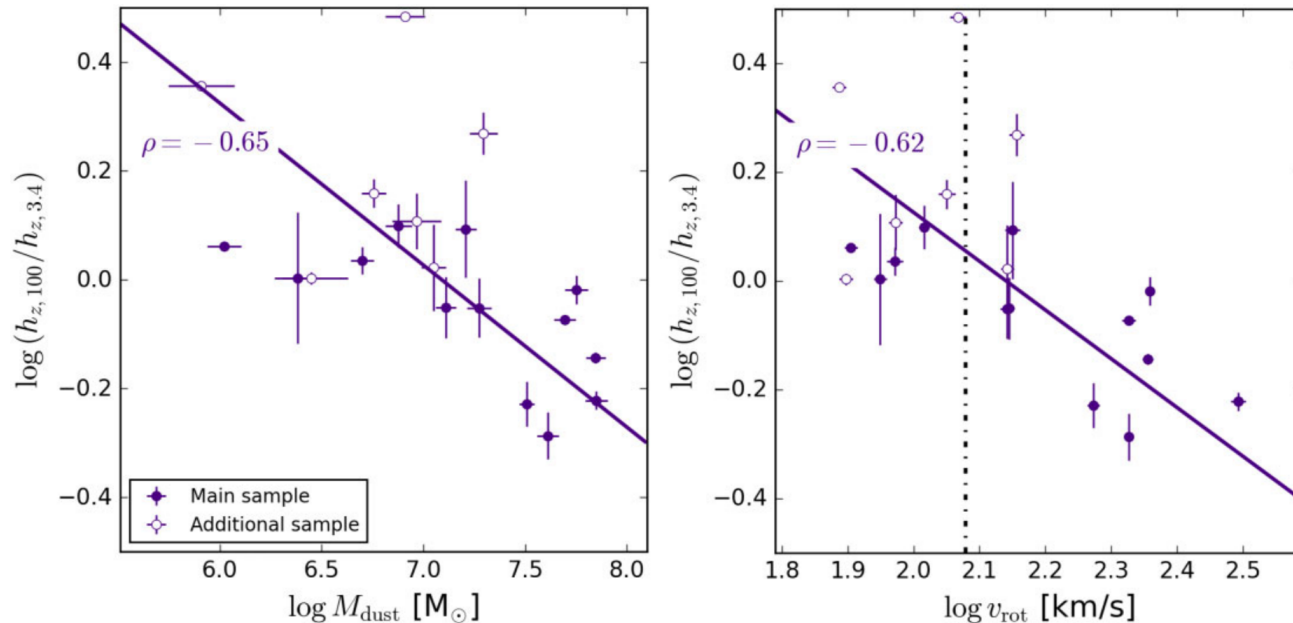in high-mass galaxies, the dusty ISM is concentrated in the plane of the thin disc

Figure 13. Correlations between the ratio of the scale heights at 100 and 3.4 μm and the total dust mass (upper panel) and the rotation velocity (bottom panel). The solid lines depict linear regression lines. The dash-dotted line shows 120 km s^{-1}.

Conclusions

PART.07

7. Conclusions

In this paper, they have extended the study by M19 with a main focus on the vertical structure of the dust discs using FIR/submm *Herschel* observations.
Summarize the results as follows.

✓ The obtained Sersic and 3D (broken) exponential disc models describe the observed emission profiles equally well.

✓ The effective radius of the dust emission, the disc scale length and scale height increase with wavelength, whereas the apparent flattening of the Sersic model remains almost constant.

✓ For 6 (and possibly additional four) of the 16 large galaxies in our sample, we clearly detect a second vertically extended component which can be interpreted as a thick dust disc or a halo.

✓ Similar to the stellar discs, the dust discs grow proportionally in the vertical and radial directions.

✓ We found moderate positive correlations between the disc scale lengths in the NIR and FIR and between the scale heights in the same domains, confirming that the dust mass distribution correlates with the total stellar distribution, probably through the population of AGB stars.

✓ Based on the dust emission in the FIR, we found an anticorrelation between the intrinsic flattening (relative thickness) of the dust disc and the dust mass. And the dust disc flatness and the ratio between the dust disc scale height and the stellar disc scale height anticorrelate with the maximum galaxy rotation velocity.